Rad6B Is a Positive Regulator of β-Catenin Stabilization

Malathy P.V. Shekhar,[1,2] Brigitte Gerard,[1] Robert J. Pauley,[3] Bart O. Williams,[4] and Larry Tait[1]

[1]Breast Cancer Program, Karmanos Cancer Institute; Departments of [2]Pathology and [3]Internal Medicine, Wayne State University, Detroit, Michigan; and the [4]Laboratory of Cell Signaling and Carcinogenesis, Van Andel Research Institute, Grand Rapids, Michigan

Abstract

Mutations in *β-catenin* or other Wnt pathway components that cause β-catenin accumulation occur rarely in breast cancer. However, there is some evidence of β-catenin protein accumulation in a subset of breast tumors. We have recently shown that Rad6B, an ubiquitin-conjugating enzyme, is a transcriptional target of β-catenin/TCF. Here, we show that forced Rad6B overexpression in MCF10A breast cells induces β-catenin accumulation, which despite being ubiquitinated is stable and transcriptionally active. A similar relationship between Rad6B, β-catenin ubiquitination, and transcriptional activity was found in WS-15 and MDA-MB-231 breast cancer cells, and mouse mammary tumor virus–Wnt-1 mammary tumor—derived cells, implicating Rad6B in physiologic regulation of β-catenin stability and activity. Ubiquitinated β-catenin was detectable in chromatin immunoprecipitations performed with β-catenin antibody in MDA-MB-231 but not MCF10A cells. Rad6B silencing caused suppression of β-catenin monoubiquitination and polyubiquitination, and transcriptional activity. These effects were accompanied by a reduction in intracellular β-catenin but with minimal effects on cell membrane–associated β-catenin. Measurement of β-catenin protein stability by cycloheximide treatment showed that Rad6B silencing specifically decreases the stability of high molecular β-catenin with minimal effect upon the 90-kDa nascent form. *In vitro* ubiquitination assays confirmed that Rad6B mediates β-catenin polyubiquitination, and ubiquitin chain extensions involve lysine 63 residues that are insensitive to 26S proteasome. These findings, combined with our previous data that *Rad6B* is a transcriptional target of β-catenin, reveal a positive regulatory feedback loop between Rad6B and β-catenin and a novel mechanism of β-catenin stabilization/activation in breast cancer cells. [Cancer Res 2008;68(6):1741–50]

Introduction

The *Rad6* gene encodes a 17-kDa ubiquitin-conjugating enzyme (UBC; refs. 1–3) that covalently adds ubiquitin to selected lysine residues of proteins. Rad6 is required for several functions, including DNA repair, and induced mutagenesis (4–6). The UBC activity is essential for Rad6 function because replacement of the conserved Cys88 with Ser produces a null phenotype (7, 8). Two closely related human homologues of yeast *Rad6, HHR6A* and *HHR6B* (referred as *Rad6A* and *Rad6B*), encode UBC enzymes and complement the DNA repair and UV mutagenesis defects of the *S. cerevisiae rad6* mutant (9, 10). The requirement for at least one functional *Rad6A* or *Rad6B* allele in all somatic cell types is supported by the fact that male and female mice lacking both homologues are nonviable (11). Rad6B expression levels are low in normal human breast tissues; however, increases are observed in breast hyperplasias and overexpression in breast carcinomas (12). *Rad6B* is a transcriptional target of β-catenin/T-cell factor (TCF; ref. 13), and its expression is subject to negative regulation in normal breast cells. Derepression and/or activation of the *Rad6B* promoter require coexpression of p300 and β-catenin (13).

Cell membrane–associated β-catenin serves a structural role within the intercellular adherens junctions, whereas cytoplasmic/nuclear β-catenin acts as a transcription cofactor in concert with the TCF/LEF family of DNA-binding proteins (14). Elevated β-catenin levels in the cytoplasm/nucleus of tumor cells are suggestive of β-catenin stabilization and can result in enhanced β-catenin–mediated transcriptional activity (15). Cytoplasmic β-catenin levels are regulated by phosphorylation on serine/threonine residues through glycogen synthase kinase 3 β in a multiprotein complex with axin and adenomatous polyposis coli (16, 17). This results in low β-catenin levels due to ß-Transducin repeat–containing proteins (βTrCP)-mediated ubiquitin-proteasomal degradation (16). The activity of this complex is negatively regulated by Dishevelled-1 resulting in β-catenin stabilization, nuclear translocation, and induction of TCF target gene expression (17, 18). Mutations in *β-catenin* or other Wnt pathway components, which result in β-catenin accumulation, are found in many human cancers but only rarely in breast cancer. However, there is some evidence of β-catenin accumulation in human breast tumors (19). Activated Wnt signaling leads to mammary tumorigenesis in mouse mammary tumor virus (MMTV)-Wnt-1 transgenic mice (20, 21).

Here, we examined the relationship between Rad6B expression and β-catenin ubiquitination/stability/transcriptional activity in breast cancer models using constitutive overexpression and silencing strategies. *In vitro* ubiquitination assays confirmed that β-catenin is a substrate for Rad6B-mediated polyubiquitination, and ubiquitin–β-catenin conjugates generated by recombinant Rad6B are insensitive to 26S proteasome. Our data reveal a novel mechanism for β-catenin stabilization in breast cancer cells.

Materials and Methods

Cells and culture conditions. MCF10A and MCF10A cells stably expressing wild-type, catalytically inert (C88A) mutant *Rad6B* or empty vector, and WS-15 breast cancer cells (22) were cultured as previously described (12). MDA-MB-231, SW480, and G177 were maintained in DMEM/F-12 medium supplemented with 5% fetal bovine serum. G177 epithelial cultures were established from a 5-month-old MMTV-Wnt-1 mouse mammary tumor (21) and characterized by cytokeratin staining. Cells were treated with the proteasome inhibitor MG-132 (25 μmol/L; Calbiochem) 5 h before lysate preparation.

Details concerning source of antibodies, reverse transcription-PCR (RT-PCR), Western blot, assessment of ubiquitination status, Chromatin

Requests for reprints: Malathy P.V. Shekhar, Breast Cancer Program, Karmanos Cancer Institute, 110 East Warren Avenue, Detroit, MI 48201. Phone: 313-578-4326; Fax: 313-831-7518; E-mail: shekharm@karmanos.org.

doi:10.1158/0008-5472.CAN-07-2111

immunoprecipitation (ChIP) assays, and statistical analysis are provided as Supplementary Materials and Methods.

ShRNA knockdown and reporter assays. Rad6B shRNA plasmid driven by human U6 promoter and targeting five different sites (nucleotides 454–474, 489–509, 287–307, 152–172, and 387–407) of murine Rad6B mRNA were purchased from Sigma Chemicals. ShRNAs targeting 489 to 509, 287 to 307, and 152 to 172 of mouse Rad6B mRNA are compatible for targeting human Rad6B mRNA. Cells were transfected with 1 μg of Rad6BshRNA or empty pLKO.1-puro vector using Metafectene (Biontex Laboratories GmbH). At 48 h, cells were subjected to a second round of transfection and, 48 h later, lysed for RT-PCR or Western blot analysis. WS-15 cells were also stably transfected with empty vector or Rad6BshRNA#4, stable pools selected with puromycin, and used for subcellular fraction analysis.

To assay the transcriptional activity of TCF/β-catenin, MCF10A, MCF10A-Rad6B, MDA-MB-231, or SW480, cells were cotransfected with 1 μg pTOP/FLASH or pFOP/FLASH (Upstate Biotech) and 100 ng of pRLTK (Promega) vectors. For all cotransfection experiments, the total mass of DNA was kept constant with appropriate amounts of the respective control vectors. Reporter activity was measured with Promega Dual Luciferase Assay system and firefly luciferase activity normalized against Renilla luciferase. Triplicate dishes were assayed for each transfection, and three to four independent transfection assays were performed.

Measurement of protein stability. WS-15 cells were transiently transfected with empty vector or Rad6BshRNA as described above, and 24 h after the second round of transfection, cells were treated with cycloheximide (30 μg/mL) to inhibit *de novo* protein synthesis. Rad6 and β-catenin (nascent and high Mr forms) levels relative to β-actin in cytosols of untreated and cycloheximide-treated cells were detected by Western blotting and semiquantified by scanning densitometry and MCID Elite software.

Ubiquitination assays. Histone H2A ubiquitination was assessed in WS-15 cells transiently transfected with empty or Rad6B shRNA #4 vector. Extracts were incubated at 37°C for 1 h with histone H2A (2.5 μg; Roche Biotech), ubiquitin-activating enzyme estrone (E1; 50 μg/mL; BioMol), ubiquitin (1.25 mg/mL), 2 mmol/L $MgCl_2$, 4 mmol/L ATP, and energy regeneration system (ERS; BostonBiochem) in reaction buffer [50 mmol/L Tris-HCl (pH 7.5)]. Some reactions were performed in the absence of ATP and ERS. In some reactions, rRad6B (85 μg/mL; BostonBiochem) was substituted for WS-15 cell extracts and served as a positive control. Reactions were subjected to SDS-PAGE and immunoblotted with ubiquitin antibody. The ability of Rad6B to ubiquitinate glutathione *S*-transferase (GST)-tagged β-catenin *in vitro* was determined using E1, rRad6B (85 μg/mL), wild-type, methylated, K48R, or K63R ubiquitin (1.25 mg/mL; BostonBiochem), 2 mmol/L ATP, and GST–β-catenin (50 μg/mL). To determine the susceptibility of Rad6B-ubiquitinated GST–β-catenin to 26S proteasomal degradation, preformed ubiquitin–β-catenin conjugates (1/10th of reaction) were incubated at 30°C for 45 min with 100 nmol/L purified 26S proteasome fraction (BostonBiochem) and 1 mmol/L ATP. Reactions were subjected to SDS-PAGE and immunoblotted with ubiquitin or GST antibody. The activity of 26S proteasomal fraction was determined by measuring hydrolysis of the proteasome-specific peptide Suc-Leu-Leu-Val-Tyr-AMC (Suc-LLVY-AMC; 25 nmol/L; BostonBiochem) using a Hitachi 2000 fluorescence spectrophotometer. The specificity of the 26S proteasome–mediated hydrolysis was confirmed by preincubating 26S proteasome fraction with a 10-fold excess of the proteasomal inhibitor, clasto-Lactacystin β-lactone (CLβL; BostonBiochem).

Three-dimensional morphogenesis assays. MCF10A-Neo or MCF10A-Rad6B cells (1×10^5) were mixed with an equal volume of 2% Matrigel (Collaborative Research) and plated on 100% Matrigel-coated eight-chambered slides. Cultures were fed every 3rd day and, on day 5 to 6, fixed in buffered formalin and paraffin embedded. Sections were stained with antibodies to Rad6, β-catenin, proliferating cell nuclear antigen (PCNA), or epithelial mucin antigen (EMA) followed by biotinylated secondary antibody and horseradish peroxidase–conjugated streptavidin.

Immunostaining. For immunofluorescence staining, cells were grown on coverslips, fixed in methanol/acetone (1:1, v/v), and incubated with Rad6B and β-catenin antibodies followed by FITC- or Texas red–conjugated secondary antibodies (Molecular Probes). Slides were counterstained with 4′,6-diamidino-2-phenylindole (DAPI), and images were captured with BX60 Olympus microscope. To determine the effect of Rad6B silencing on β-catenin levels/localization and cyclin D1, WS-15 cells transfected with empty or Rad6B shRNA# 4 vector were stained with Rad6, β-catenin, or cyclin D1 antibodies. Sections of Wnt-1 mammary tumors or virgin normal mammary glands were incubated with Rad6 or β-catenin antibodies, and

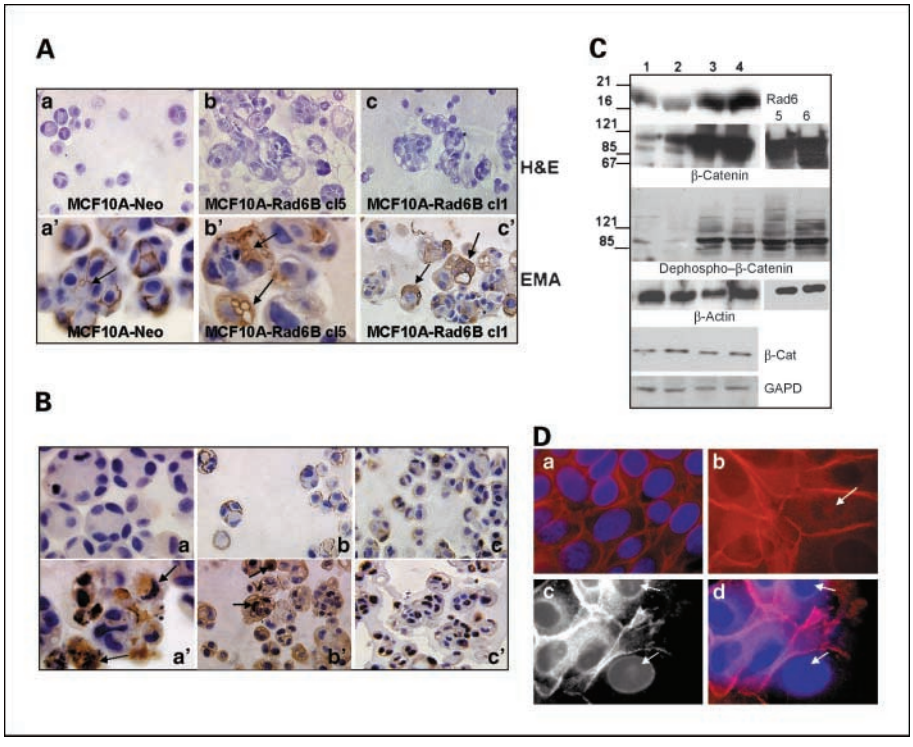

Figure 1. Constitutive Rad6B overexpression induces loss of epithelial polarity and up-regulation of β-catenin. *A,* epithelial acini were stained with H&E (*a–c*) or EMA antibody (*a′–c′*). *B,* epithelial acini stained with antibodies to Rad6 (*a* and *a′*), β-catenin (*b* and *b′*), or PCNA (*c* and *c′*). Magnification, ×10 (*Aa–Ac* and *Ac′*; *Bb, Bb′, Bc*, and *Bc′*); ×40 (*Aa′, Ab′, Ba*, and *Ba′*). *C,* steady-state levels of Rad6, β-catenin, and dephospho-β-catenin-33/37/41 in MCF10A-Neo (*lane 1*); MCF10A-Rad6B clone 2 (*lane 2*), MCF10A-Rad6B clone 1 (*lane 3*), and MCF10A-Rad6B clone 5 (*lane 4*) cells, and β-catenin and dephospho-β-catenin in MDA-MB-231 (*lane 5*) and SW-480 (*lane 6*) total cell lysates relative to β-actin. *Bottom,* semiquantitative RT-PCR analysis of β-catenin and GAPD expression in MCF10A-Neo (*lane 1*), MCF10A-Rad6B clone 2 (*lane 2*), MCF10A-Rad6B clone 1 (*lane 3*), and MCF10A-Rad6B clone 5 (*lane 4*) cells. *D,* immunofluorescence staining of β-catenin in MCF10A-Neo (*a*), MCF10A-Rad6B clone 1 (*b*), and clone 5 (*c* and *d*) cells. *c* is a black and white transformation of *d. Arrows,* nuclear staining for β-catenin. *a* and *d* were counterstained with DAPI. Magnification, ×25.

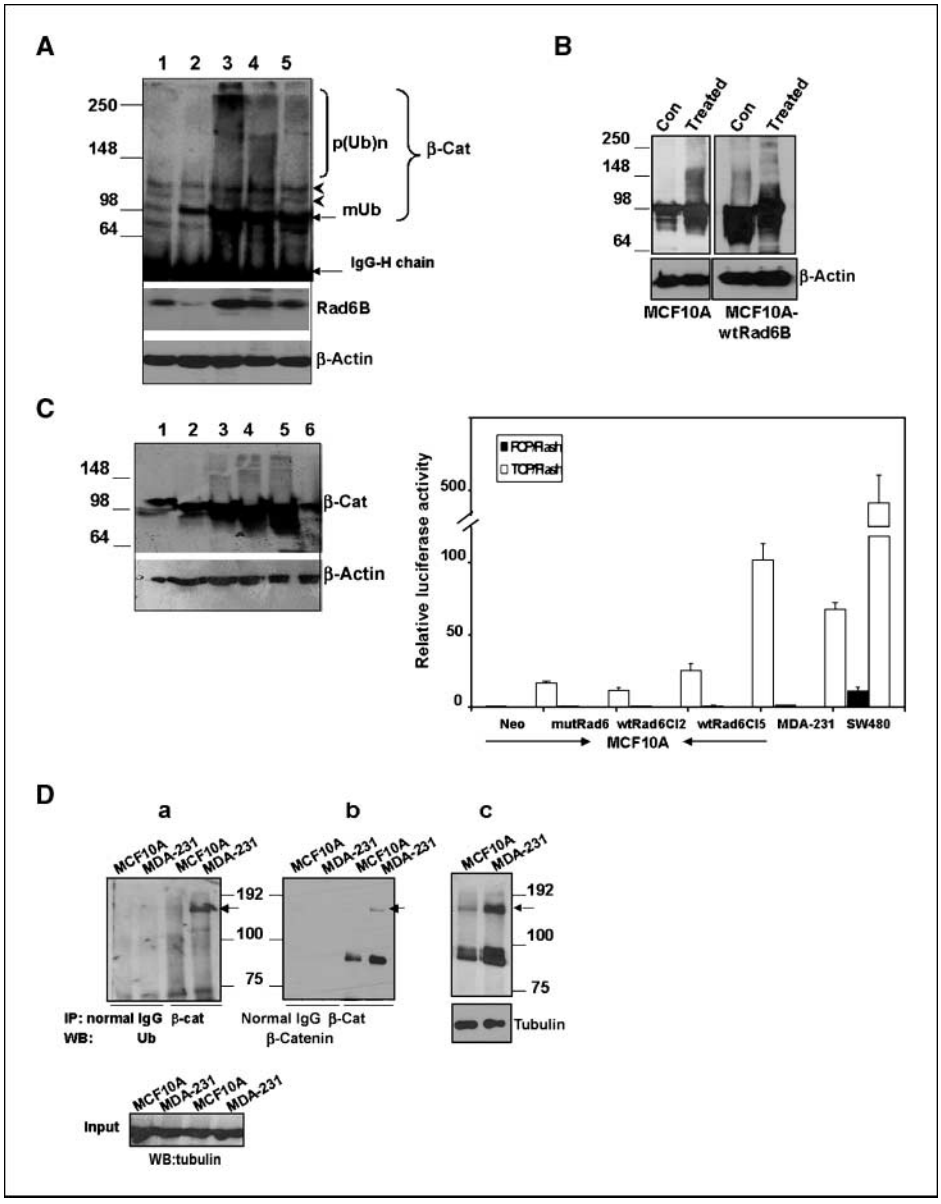

Figure 2. β-catenin protein is ubiquitinated in Rad6B-overexpressing MCF10A cells. *A,* cytosolic extracts were immunoprecipitated (*IP*) with β-catenin antibody and Western blotted with conjugated ubiquitin-reactive FK2 antibody. *Lane 1,* MCF10A-mutant *rad6B*; *lane 2,* MCF10A-Neo; *lane 3,* MCF10A-Rad6B clone 5; *lane 4,* MCF10A-Rad6B clone 1; and *lane 5*, MDA-MB-231 cells. Regions corresponding to the monoubiquitinated (*mUb*)and polyubiquitinated (*pUbn*) forms of β-catenin (*β-cat*) are indicated. *Arrowheads,* note that the ubiquitinated β-catenin bands are not influenced by Rad6B. *Bottom,* corresponding levels of Rad6 and β-actin are shown in the panels. *B,* steady-state levels of total β-catenin in control and MG-132–treated MCF10A-Neo or MCF10A-Rad6B clone 5 cells. *C,* steady-state levels of β-catenin in MCF10A-Neo (*lane 1*), MCF10A-Rad6B clone 2 (*lane 2*), MCF10A-Rad6B clone 5 (*lane 3*), MDA-MB-231 (*lane 4*), SW480 (*lane 5*), and MCF10A-mutant *rad6B* (*lane 6*) whole cell lysates. *Right,* transcriptional activity of β-catenin. Luciferase activity from TOP/Flash or FOP/Flash vectors were normalized against Renilla luciferase. *Columns,* mean of four independent experiments; *bars,* SE. *D,* ChIPs were performed on MCF10A or MDA-MB-231 cells with anti–β-catenin antibody or nonimmune IgG followed by Western blotting with ubiquitin (*a*) or β-catenin antibody (*b*). *b,* reactivity of stripped membrane from *a* to β-catenin antibody. Equal input was verified by immunoblotting with tubulin antibody. *c,* steady-state levels of β-catenin in the extracts used for ChIP. *Arrows,* position of β-catenin bands (*b* and *c*) that are immunoreactive to ubiquitin antibody (*a*).

appropriate secondary antibody. Controls included isotype-matched murine or rabbit antibodies of irrelevant specificity. Data obtained from counting triplicates of 100 cells were averaged.

Results

Constitutive Rad6B overexpression induces up-regulation of β-catenin and loss of epithelial polarity. We have previously shown that forced Rad6B overexpression in MCF10A cells induces hyperplastic lesion formation *in vivo* (13). To define the role of Rad6B in early breast cancer, we examined the effect of Rad6B overexpression on epithelial polarity. Whereas MCF10A-Neo cells organize into acini containing a polarized epithelium and well-defined central lumen as detected by EMA staining (Fig. 1*Aa, Aa'*, and *Ba*), similar cultures of MCF10A-Rad6B clones 1 or 5 produce disorganized structures (Fig. 1*Ab* and *Ac*) that lack central lumen or contain asymmetrical lumen (Fig. 1*Ab'* and *Ac'*). Consistent with chromosomal instability of MCF10A-Rad6B cells (12), MCF10A-Rad6B acini display nuclear pleiomorphism (Fig. 1*Ba'*) compared with uniform nuclei of MCF10A-Neo cells (Fig. 1*Ba*). Unlike in MCF10A-Neo acini, β-catenin is not confined to the cell membranes in MCF10A-Rad6B acini but shows strong cytoplasmic reactivity (Fig. 1*B*; compare *b* and *b'*). Diffuse nuclear staining for β-catenin was observed in cells displaying intense cytoplasmic staining (Fig. 1*Bb', arrows*). Unlike MCF10A-Neo acini, MCF10A-Rad6B acini are proliferative as >30% of cells are PCNA positive (Fig. 1*B*; compare *c* and *c'*).

Immunoblot analysis of MCF10A-Rad6B and MCF10A-Neo whole cell lysates showed that MCF10A-Rad6B clones 1 and 5 that expressed ~10- to 20-fold higher levels of Rad6B, respectively, also expressed approximately >15-fold higher levels of β-catenin compared with MCF10A-Neo cells. Immunoblotting with dephospho-β-catenin antibody confirmed that a notable proportion of β-catenin in MCF10A-Rad6B cells is unphosphorylated (Fig. 1*C*). β-catenin expression was further confirmed by immunofluorescence staining, which showed intense cytoplasmic β-catenin staining in MCF10A-Rad6B cells as opposed to the localized

membrane staining in MCF10A-Neo cells (Fig. 1*D*; compare *a* with *b–d*). Again, as observed in three-dimensional acini (Fig. 1*Bb'*), diffuse nuclear β-catenin staining was detected (Fig. 1*D, b–d, arrows*). However, because MCF10A-Rad6B cells pile up (Fig. 1*Db* and *Dd*), the percent of cells showing nuclear β-catenin could not be accurately estimated. Evidence for the presence of nuclear β-catenin in MCF10A-Rad6B cells was obtained by analysis of subcellular fractions as shown later in the text. β-catenin accumulation in MCF10A-Rad6B clones resulted from increased protein stability rather than transcriptional induction, as no changes in β-catenin mRNA levels relative to glyceraldehyde-3-phosphate dehydrogenase (GAPD) were detected by semiquantitative RT-PCR (Fig. 1*C, bottom*).

Up-regulated β-catenin protein is ubiquitin conjugated and displays increased transcriptional activity. To determine whether β-catenin in MCF10A-Rad6B cells (Fig. 1*Bb', C*, and *D*) exhibits alterations in posttranslational ubiquitin modifications, cytosols of MCF10A-wild-type Rad6B clones, MCF10A-mutant *rad6B*, or MCF10A-Neo cells were immunoprecipitated with β-catenin antibody and immunoblotted with FK2 antibody (23). Similar analysis was performed with MDA-MB-231 cells because they naturally express high levels of E-cadherin–uncomplexed β-catenin (24). Monoubiquitinated β-catenin protein levels were >5-fold higher in MDA-MB-231 and MCF10A-Rad6B clones 1 and 5 compared with MCF10A-Neo cells (Fig. 2*A*). Monoubiquitinated β-catenin levels were dramatically reduced in MCF10A-mutant *rad6B* cells compared with MCF10A-Neo cells (Fig. 2*A*; band indicated by arrow in *lanes 1* and *2*). The intensities of two other FK2-reactive β-catenin bands (Fig. 2*A, arrowheads*) failed to show similar correlations with Rad6 protein levels, suggesting that these β-catenin ubiquitination events are probably not mediated by Rad6B. Polyubiquitinated β-catenin was detected as a high Mr smear in MCF10A-Rad6B clones 1, 5, and MDA-MB-231 cells and was absent in MCF10A-Neo and MCF10A-mutant *rad6B* cells (Fig. 2*A*; compare *lanes 1* and *2* with *3, 4*, and *5*). These data suggest that Rad6B may regulate both β-catenin monoubiquitination and polyubiquitination. These results were verified by assessing the effect of 26S proteasomal inhibitor MG-132 on β-catenin steady-state levels in MCF10A and MCF10A-Rad6B clone 5 cells. MG-132 treatment caused accumulation of nascent and high Mr β-catenin forms in MCF10A cells. Similar treatment of MCF10A-Rad6B clone 5 cells caused further polyubiquitination as observed by an upward shift in the β-catenin–reactive bands compared with untreated MCF10A-Rad6B cells (Fig. 2*B*).

To determine whether the endogenous β-catenin in MCF10A-Rad6B cells is functionally active, transient reporter assays were performed with pTOP/Flash reporter construct. MCF10A-Rad6B clones displayed ~5- (clone 1; data not shown) to 6-fold (clone 5) higher levels of reporter activity, respectively, compared with MCF10A-Neo cells (Fig. 2*C, right*). SW480 cells, which express high

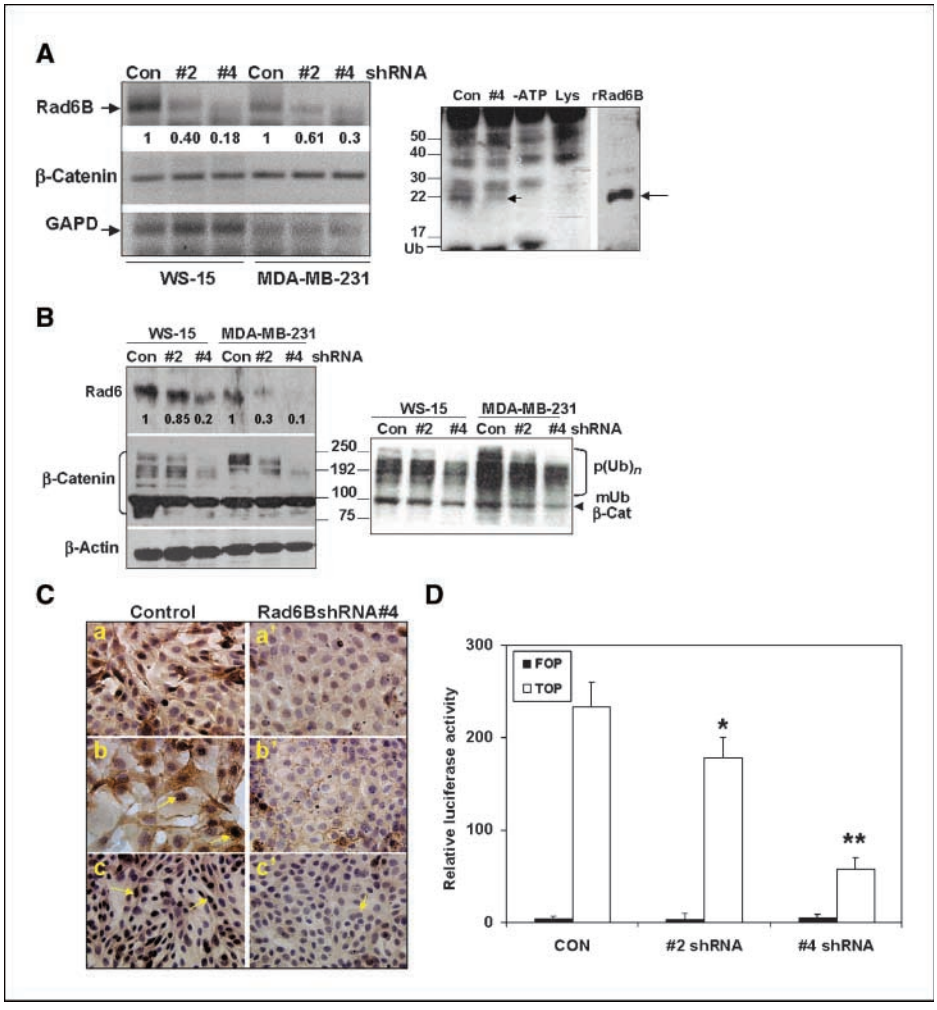

Figure 3. β-catenin ubiquitination is suppressed by Rad6B silencing. *A,* semiquantitative RT-PCR analysis of Rad6B, β-catenin, and GAPD expression in WS-15 or MDA-MB-231 cells transfected with control (*con*) or Rad6BshRNA#2- or Rad6BshRNA#4-encoded vectors. *Right,* Rad6B-depleted cells display diminished histone H2A ubiquitin-conjugating activity. Reactions were performed with empty vector (*con*) or Rad6BshRNA#4-transfected WS-15 cell extracts. Recombinant Rad6B was used as a positive control. Reactions lacking ATP (*−ATP*) were included to assess the specificity of the reactions. *Lys,* WS-15 cell extracts not exposed to ubiquitination reaction. *Arrow,* position of monoubiquitinated histone H2A. *B,* cytosolic steady-state levels of Rad6 or β-catenin protein relative to β-actin in control or Rad6BshRNA-transfected cells. *Right,* cytosolic extracts containing equivalent amounts of total protein were immunoprecipitated with β-catenin antibody and immunoblotted with FK2 antibody. *C,* Rad6B depletion results in decline in intracellular levels of β-catenin. WS-15 cells transfected with empty vector (*control*) or Rad6B shRNA #4 were immunostained with Rad6 (*a* and *a'*), β-catenin (*b* and *b'*), or cyclin D1 (*c* and *c'*) antibodies. *Arrows,* nuclei showing positive reactivities. Magnification, ×25 (*a, a', b', c*, and *c'*); ×40 (*b*). *D,* Rad6B depletion induces suppression of β-catenin–mediated transcriptional activation from TOP/FLASH reporter construct in WS-15 cells. Activity was normalized against Renilla luciferase activity. *Columns,* mean of four independent experiments; *bars,* SE. * and **, significant decreases in luciferase activity in Rad6BshRNA#2 ($P < 0.01$) and Rad6BshRNA#4 ($P < 0.001$) compared with vector control cells.

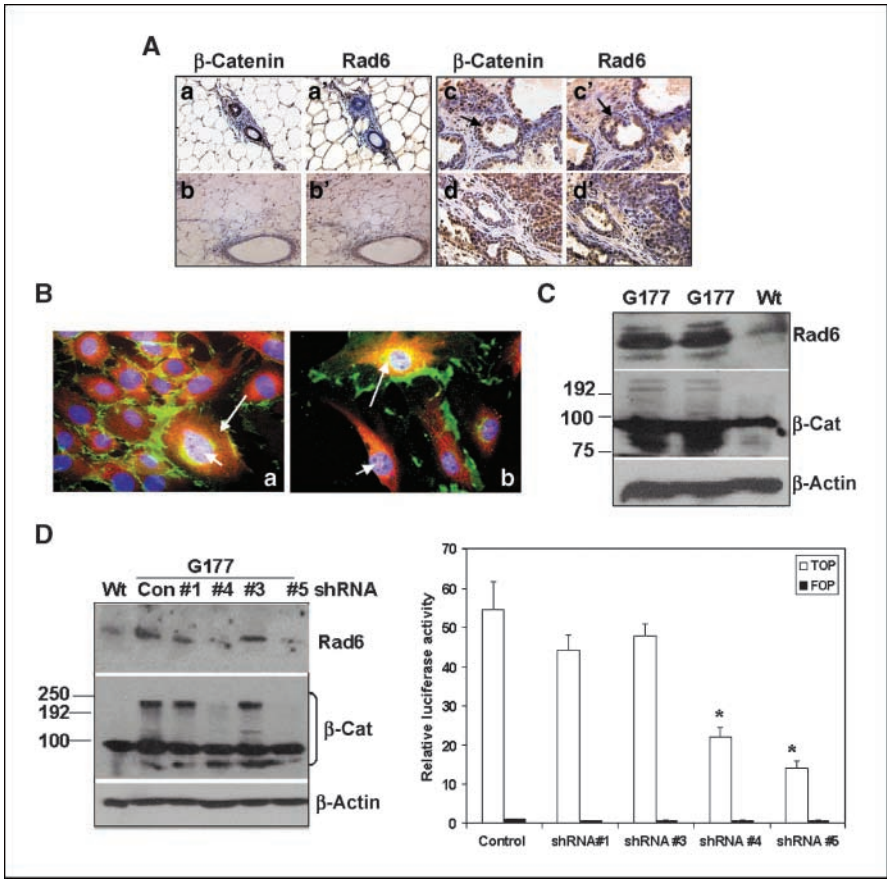

Figure 4. *A,* Rad6 is overexpressed in mammary tumors of MMTV-Wnt-1 transgenic mice. Immunohistochemical analysis of Rad6 and β-catenin in normal (*a, a', b*, and *b'*) and Wnt-1 transgenic (*c, c', d*, and *d'*) mammary glands. *a, a'*, and *b, b',* mammary glands at 5 wk and 5 mo, respectively; *c* and *c'* (hyperplastic), and *d* and *d'* (invasive carcinoma), mammary glands at 15 wk. Magnification, ×10 (*a, a', b*, and *b'*); ×25 (*c, c', d*, and *d'*). *B,* Rad6 (*red*) and β-catenin (*green*) show physical colocalization in cytoplasm (*long arrow*) and/or nuclei (*short arrow*) of G177 cultures at confluence (*a*) and sparse (*b*) cell densities. *C,* steady-state levels of Rad6 and β-catenin relative to β-actin in whole cell lysates of G177 and wild-type mammary epithelial cultures. *D,* steady-state levels of β-catenin and Rad6 in G177 cytosolic extracts after transfection with control or Rad6B shRNA–encoded vectors. *Wt,* wild-type mammary cells. *Right,* Rad6B depletion induces decrease in β-catenin–mediated transcriptional activity from TOP/FLASH reporter vector. Activity was normalized against Renilla luciferase activity. *Columns,* mean of three independent experiments; *bars,* SE. *, significant decreases ($P < 0.01$) compared with vector control cells.

levels of endogenous β-catenin (Fig. 2*C, lane 5*), showed >20- fold higher levels, and MDA-MB-231 cells showed ~4-fold higher levels of TOP activity compared with MCF10A-Neo cells (Fig. 2*C, right*). Transfection with pFOP/Flash vector yielded minimal activity (Fig. 2*C, right*). These data suggest that ubiquitin-modified β-catenin in MCF10A-Rad6B cells is transcriptionally active.

To determine the presence of ubiquitinated β-catenin on chromatin, we performed ChIP assays with β-catenin antibody followed by immunoblotting with ubiquitin antibody. An intense ~160-kDa ubiquitin-immunoreactive band was detected in MDA-MB-231 cells but not in MCF10A cells (Fig. 2*Da*). Similar probing of nonimmune IgG ChIP failed to show ubiquitin reactivity (Fig. 2*Da*). Reprobing of the stripped membrane with β-catenin antibody authenticated the presence of β-catenin in the ubiquitin-reactive ~160-kDa band (Fig. 2*Db, arrow*). The inability to detect ubiquitinated β-catenin from MCF10A cells is not due to inefficient ChIP but rather to its presence in trace amounts, as similar differences in the proportions of unmodified β-catenin between MCF10A and MDA-MB-231 cells were detected in ChIPs and extracts used for ChIP assays (Fig. 2*D*; compare *b* and *c*). The steady-state level of the 160-kDa ubiquitinated β-catenin band was ~14-fold higher in MDA-MB-231 cells compared with MCF10A cells (Fig. 2*D, Dc*). These data suggest that ubiquitinated β-catenin is associated with chromatin.

Rad6B silencing inhibits β-catenin ubiquitination and decreases β-catenin transcriptional activity. Because our results from MCF10A-Rad6B cells showed a direct association between Rad6B levels and β-catenin ubiquitination status, we assessed the physiologic relevance of Rad6B in β-catenin ubiquitination. Human breast cancer cells (WS-15 and MDA-MB-231) and MMTV-Wnt-1 transgenic mouse mammary tumor model that show elevated levels of endogenous β-catenin were used.

Human breast cancer cells. WS-15 and MDA-MB-231 cells were transiently transfected with Rad6B shRNA #2 or #4 or the empty vector, and efficacy of Rad6B silencing was determined by semiquantitative RT-PCR and Western blot analysis. Rad6B mRNA levels relative to GAPD mRNA were reduced robustly in WS-15 or MDA-MB-231 transfected with Rad6B shRNA#4 compared with control vector (Fig. 3*A*). Consistent with the RT-PCR data, Rad6B shRNA#4 caused a commensurate decrease in Rad6B protein levels in WS-15 and MDA-MB-231 cells (Fig. 3*B*). Simultaneous measurement of β-catenin protein levels in the same extracts showed that Rad6B-depleted extracts also displayed a coincident decrease in high Mr β-catenin forms with minimal effects on the ~90-kDa nascent protein (Fig. 3*B*). These data are consistent with RT-PCR data that showed that Rad6B suppression does not influence β-catenin transcription (Fig. 3*A*). To confirm whether the high Mr β-catenin–reactive bands are ubiquitinated β-catenin, WS-15 or MDA-MB-231 cytosols were immunoprecipitated with β-catenin antibody, and the immunocomplexes were analyzed with FK2 antibody (23). Results of Fig. 3*B* (*right*) show that the β-catenin–reactive high Mr bands in Fig. 3*B* are ubiquitinated β-catenin, and that Rad6B depletion causes inhibition of β-catenin polyubiquitination and monoubiquitination in WS-15 and MDA-MB-231 cells. Rad6B is major ubiquitinator of histone H2A and H2B (25). To verify the effect of Rad6B depletion on its UBC activity, histone H2A ubiquitination assays were performed in extracts of Rad6B shRNA#4 or empty vector–transfected WS-15 cells. As

shown in Fig. 3*A* (*right*), histone H2A monoubiquitination (*arrow*) was markedly reduced in Rad6B-silenced WS-15 compared with control lysates. Ubiquitinated histone H2A was not detected in reactions lacking ATP, and an intense monoubiquitinated histone H2A band was detected in parallel reactions containing rRad6B (Fig. 3*A, right, arrow*).

To further confirm that Rad6B silencing results in decrease in intracellular β-catenin, immunocytochemical analysis of Rad6 and β-catenin was performed in WS-15 cells. Rad6B staining was detected in the cytoplasm and/or nuclei of control vector–transfected WS-15 cells (Fig. 3*Ca*). β-catenin immunoreactivity was detected on the membranes, cytoplasm, and in ~1% to 5% of the nuclei of WS-15 cells (Fig. 3*Cb*), along with intense nuclear staining for cyclin D1 (Fig. 3*Cc*). Rad6B depletion (Fig. 3*C*; compare *a* and *a'*) induced a dramatic drop in both β-catenin (Fig. 3*C*; compare *b* and *b'*) and cyclin D1 (Fig. 3*C*; compare *c* and *c'*) staining but had less influence on cell membrane–associated β-catenin. Control WS-15 cells grow as loosely packed and piled-up colonies, whereas Rad6B-silenced WS-15 cells grow as discrete monolayer with tight cell-cell adherens junctions (Fig. 3*C*; compare *b* and *b'*). Rad6B depletion caused a dramatic drop in intracellular β-catenin reactivity and potentially offers an explanation for the observed decrease in cyclin D1 expression (26) in WS-15-Rad6BshRNA cells. Because Rad6B suppression induced a decrease in ubiquitinated β-catenin forms (Fig. 3*B*), we evaluated the consequence of reduced β-catenin ubiquitination on its transcriptional activity. WS-15-Rad6BshRNA#4 cells showed an ~3-fold decrease in TOP-mediated reporter activity compared with vector controls (Fig. 3*D*). These findings indicate that Rad6B expression levels can significantly influence β-catenin ubiquitination and consequently regulate its levels, stability, and activity.

Wnt-1 transgenic mammary tumor model. The functional role of Rad6B on β-catenin modification and transcriptional activity was also evaluated in MMTV-Wnt-1 mammary tumor model because mammary tumorigenesis in this system is dependent on activation of β-catenin signaling (27, 28). Immunohistochemical staining of Wnt-1 mammary hyperplasias (Fig. 4*Ac* and *Ac'*) and invasive carcinomas (Fig. 4*Ad* and *Ad'*) showed intense nuclear and cytoplasmic staining for β-catenin (Fig. 4*Ac* and *Ad*) and Rad6 (Fig. 4*Ac'* and *Ad'*). Similar analysis of normal mammary tissues at 5 weeks (Fig. 4*Aa* and *Aa'*) and 5 months (Fig. 4*Ab* and *Ab'*) showed only weak immunoreactivity. Immunofluorescence staining of Wnt-1 mammary tumor–derived G177 cells with Rad6 and β-catenin antibodies showed the presence of high levels of Rad6 and β-catenin in the cytoplasm (Fig. 4*Ba* and *Bb, long arrow*) and/or nucleus (Fig. 4*Ba* and *Bb, short arrow*) as well as colocalization in ~25% of cells. Western blot analysis confirmed that G177 cells express substantially higher steady-state levels of Rad6 and β-catenin compared with normal mammary epithelial cells (Fig. 4*C*).

To determine whether Rad6B exerted similar positive effects on β-catenin ubiquitination and functional activity in Wnt1-tumor–derived G177 cells as with WS-15 and MDA-MB-231 cells, G177 cells were transfected with the empty vector or Rad6B shRNAs #1, 3, 4, or 5 and cytosols analyzed for Rad6 and β-catenin steady-state levels. Rad6BshRNAs caused a marked decrease in Rad6 protein levels in G177 cells (Fig. 4*D*). Rad6B silencing induced a commensurate decrease in β-catenin–reactive high Mr forms but had minimal effect upon nascent ~90-kDa β-catenin (Fig. 4*D*). These data further provide evidence that Rad6B influences only the posttranslational modification of β-catenin. Rad6B suppression

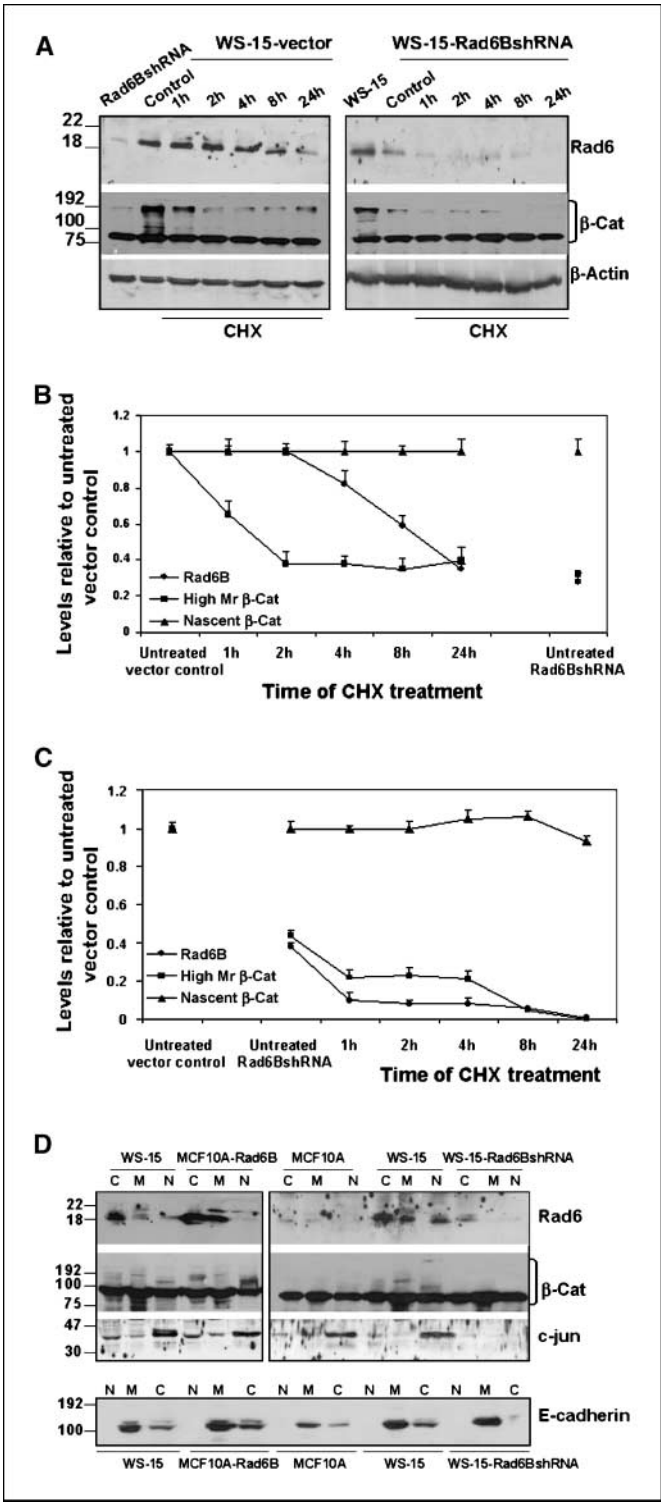

Figure 5. Stability of high Mr β-catenin is sensitive to Rad6B-silencing. WS-15 cells were transiently transfected with empty vector or Rad6BshRNA#4 and treated with cycloheximide (*CHX*; 30 μg/mL) for the indicated time intervals. *A,* steady-state levels of Rad6, β-catenin, and β-actin. *B* and *C,* graphic representation of Rad6 and β-catenin (nascent 90-kDa or high Mr regions) levels normalized to β-actin in vector control (*B*) or Rad6BshRNA (*C*) cells. *Points,* mean of two independent experiments relative to untreated vector control cells; *bars,* SE. *D,* subcellular fractions exhibit differences in high Mr modified forms of β-catenin. Steady-state levels of Rad6, β-catenin, c-jun, or E-cadherin in the cytoplasmic (*C*), membrane (*M*), or nuclear (*N*) subfractions of vector control MCF10A or WS-15 relative to their counterparts, MCF10A-Rad6B and WS-15-Rad6BshRNA#4 cells, respectively.

induced a 4- to 6-fold decrease in pTOP/Flash reporter activity compared with vector controls (Fig. 4*D, right*). These data are consistent with the results from Figs. 2 and 3, and further validate the existence of a physiologic relationship between Rad6B levels, β-catenin ubiquitination, and β-catenin–mediated transcriptional activity.

Rad6B depletion decreases the stability of high molecular weight β-catenin forms. To determine if Rad6B influences the stability of β-catenin protein, WS-15 cells were transfected with empty vector or Rad6BshRNA#4 and treated with cycloheximide to inhibit *de novo* protein synthesis. Steady-state levels of Rad6B and β-catenin proteins were analyzed in cells harvested 1 to 24 h after cycloheximide treatment and compared with untreated cells. Cycloheximide treatment reduced Rad6B protein levels in both control (half-life, >8 h; Fig. 5*A* and *B*) and Rad6BshRNA cells (Fig. 5*A* and *C*), although more quickly in the latter (half-life, <1 h). Simultaneous analysis of β-catenin in the same extracts showed that stability of nascent β-catenin molecules was relatively uninfluenced by Rad6B silencing or cycloheximide treatment within the 24 h period (Fig. 5*A*–*C*). However, the stability of high Mr β-catenin was greatly compromised in Rad6BshRNA-transfected WS-15 cells (Fig. 5*A* and *C*). Because the major decrease in high Mr β-catenin occurred in the beginning of the experiment from Rad6B silencing, this suggests that Rad6B is an important regulator of high Mr β-catenin stability. Furthermore, the cycloheximide-induced rates of decay of high Mr β-catenin paralleled that of Rad6B decay curve in Rad6BshRNA cells (Fig. 5*C*). Cycloheximide induced a sharp decline in high Mr β-catenin levels within 1 to 2 h of treatment in control cells. It is not clear if this is a result of cycloheximide-induced inhibition of Rad6B activity or is suggestive of coinvolvement of another short-lived protein.

Subcellular fractions show qualitative differences in β-catenin proteins. Because β-catenin protein showed distinct differences in its modification to higher Mr forms under conditions of Rad6B overexpression versus Rad6B silencing, we investigated whether specific qualitative and/or quantitative alterations in distribution of nascent and modified β-catenin occur in the subcellular fractions. Cytoplasmic, membrane, and nuclear fractions were prepared from MCF10A-Neo, MCF10A-Rad6B clone 5, and WS-15 cells stably transfected with Rad6BshRNA#4 or empty vector. Whereas Rad6B levels were low in all subcellular fractions of MCF10A cells, elevated levels of Rad6B were observed in the cytoplasmic fractions of MCF10A-Rad6B clone 5 and WS-15 cells (Fig. 5*D*). Nuclear Rad6B was detectable in WS-15 and MCF10A-Rad6B cells (Fig. 5*D*). Rad6B was undetectable in the membrane and nuclear fractions of WS-15-Rad6BshRNA cells and was decreased substantially in the cytoplasmic fractions compared with the empty vector–transfected WS-15 cells (Fig. 5*D*). Rad6B was present in the membrane fractions of both WS-15 and MCF10A-Rad6B cells, although at levels lower than in the cytoplasm (Fig. 5*D*). It is possible that Rad6B presence in the membrane fractions is due to cross-contamination with residual cytoplasm because c-jun was detected in the membrane and cytoplasmic fractions albeit at much lower levels compared with the corresponding nuclear fractions (Fig. 5*D*). Simultaneous analysis of β-catenin in the subcellular fractions showed the presence of nascent β-catenin in all subcellular fractions (Fig. 5*D*). However, qualitative differences in high molecular forms of β-catenin were readily visible in subcellular fractions of Rad6B-overexpressing WS-15 and MCF10A-Rad6B cells compared with their counterparts, WS-15-Rad6BshRNA and MCF10A-Neo cells, respectively (Fig. 5*D*). Although WS-15 and MCF10A-Rad6B cells displayed quantitative differences in modified β-catenin forms in the cytoplasmic and nuclear fractions, both cell lines displayed similar qualitative patterns of β-catenin modification and distribution (Fig. 5*D*). These data suggest that the observed β-catenin modifications are stable and not restricted to a cell type. The molecular sizes for cytoplasmic and nuclear-modified β-catenin ranged from ~170–190 and ~140–160 kDa, respectively. MCF10A and WS-15-Rad6BshRNA cells contained negligible amounts of modified β-catenin, although nascent β-catenin was abundantly present in all subcellular fractions (Fig. 5*D*). Immunoblot analysis of E-cadherin showed its predominant presence in the membrane fractions and complete absence in the nuclear preparations (Fig. 5*D*), further validating the significance of modified β-catenin in the nuclei of Rad6B-overexpressing cells.

Demonstration *in vitro* of Rad6B-mediated effects on β-catenin ubiquitination. Because our data showed a positive correlation between β-catenin–ubiquitin modification and Rad6B expression status, we tested whether β-catenin is a substrate for Rad6B-mediated ubiquitination. Recombinant Rad6B was incubated with purified GST–β-catenin in the presence of wild-type or methylated ubiquitin to determine if Rad6B-mediated ubiquitination involved one or more lysine residues on the β-catenin molecule. In the presence of wild-type ubiquitin, Rad6B induced β-catenin ubiquitination, and the molecular sizes of ubiquitinated β-catenin corresponded with the presence of two to four ubiquitin molecules (Fig. 6*Aa–a″*). Rad6B-mediated β-catenin ubiquitination occurs at limited residues on the β-catenin molecule because substitution of wild-type ubiquitin with methylated ubiquitin resulted in only monoubiquitination rather than multimonoubiquitination [(Fig. 6*Aa–a″*); *dotted lines,* number of ubiquitin moieties on β-catenin (*a* and *a*')]. We next tested whether Rad6B-mediated polyubiquitination involved lysine residues at positions 48 or 63 of the ubiquitin molecule because residues K48 and K63 are the major sites of chain initiation. Ubiquitination reactions were performed with K48R or K63R mutant ubiquitin, and analyzed by immunoblotting with GST or ubiquitin antibodies. As shown in Fig. 6*B*, β-catenin ubiquitination (containing 2–4 ubiquitin molecules) that was comparable with wild-type ubiquitin occurred in reactions containing K48R but not K63R ubiquitin. The GST-reactive single band observed in K63R reactions (Fig. 6*B, arrowhead*) is ubiquitinated β-catenin as it was reactive to ubiquitin antibody (Fig. 6*C*). Western blotting with ubiquitin antibody confirmed that similar extent of Rad6B-mediated β-catenin ubiquitination occurs in presence of K48R or wild-type ubiquitin (Fig. 6*C*). These data show that Rad6B-mediated β-catenin polyubiquitination involves ubiquitin chain extension by K63 linkages.

To determine whether the ubiquitinated β-catenin products are competent for 26S proteasomal degradation, an aliquot of the presynthesized ubiquitinated β-catenin conjugates generated by Rad6B were incubated with purified 26S proteasome fraction and probed with GST or ubiquitin antibodies. Incubation of ubiquitinated β-catenin conjugates generated from wild-type or K48R ubiquitin reactions with 26S proteasome showed GST reactivity localized to ubiquitinated β-catenin containing ~4 ubiquitin (~150 kDa) molecules (Fig. 6*B*, *). This GST-reactive band is not observed in K63R ubiquitin reactions exposed to 26S proteasome and suggest that it is not a contaminant from the 26S proteasome fraction. Similar analysis of 26S proteasome–treated reactions with

ubiquitin antibody showed the presence of ~150-kDa ubiquitin reactive bands in wild-type, K48R, and K63R mutant ubiquitin reactions (Fig. 6*C, arrowhead*). However, ubiquitin chain extensions originating from the 150-kDa band occurred in wild-type and K63R reactions but not in K48R reactions (Fig. 6*C*). A commensurate reactivity to the GST antibody was not detected (Fig. 6*B*). It is possible that the conversion to the 150-kDa polyubiquitinated form in K63R reactions and the heavy high Mr ubiquitin-reactive smear observed in wild-type and K63R reactions are mediated by contaminating E3 ligases in the 26S proteasome fraction (29), which unlike Rad6B, mediate chain extensions involving K48 linkages. The proteasome fraction–initiated reactions use Rad6B-initiated ubiquitin–β-catenin conjugates because incubation of input β-catenin substrate alone with 26S proteasome fraction failed to generate similar GST- (Fig. 6*B*) or ubiquitin-reactive (Fig. 6*C*) products. This decreased sensitivity of ubiquitin–β-catenin conjugates to proteasomal degradation is not due to decreased activity of the proteasomal fraction because it was functionally active toward the fluorogenic peptide substrate Suc-LLVY-AMC, and hydrolysis was inhibited by preincubation of proteasome fraction with the proteasome-specific inhibitor, CLβL (Fig. 6*D*).

Discussion

Elevated levels of β-catenin are detected in some breast cancers, suggesting an important role for β-catenin in breast carcinogenesis (30, 31), but unlike most cancers that have a high frequency of β-catenin–stabilizing mutations, mutations are rare in breast cancer (32). Described here is the first report of a direct association between Rad6B expression and β-catenin ubiquitination, and evidence of a novel mechanism for β-catenin accumulation/activation in breast cancer cells. Our data from MCF10A-Rad6B cells show that constitutive Rad6B overexpression induces ubiquitination of β-catenin protein. Despite ubiquitination, β-catenin is stable, and treatment of MCF10A-Rad6B cells with the proteasome inhibitor MG-132 causes a further increase in molecular sizes of the high Mr β-catenin forms. This relationship between Rad6B and β-catenin stabilization is not an artifact of forced Rad6B

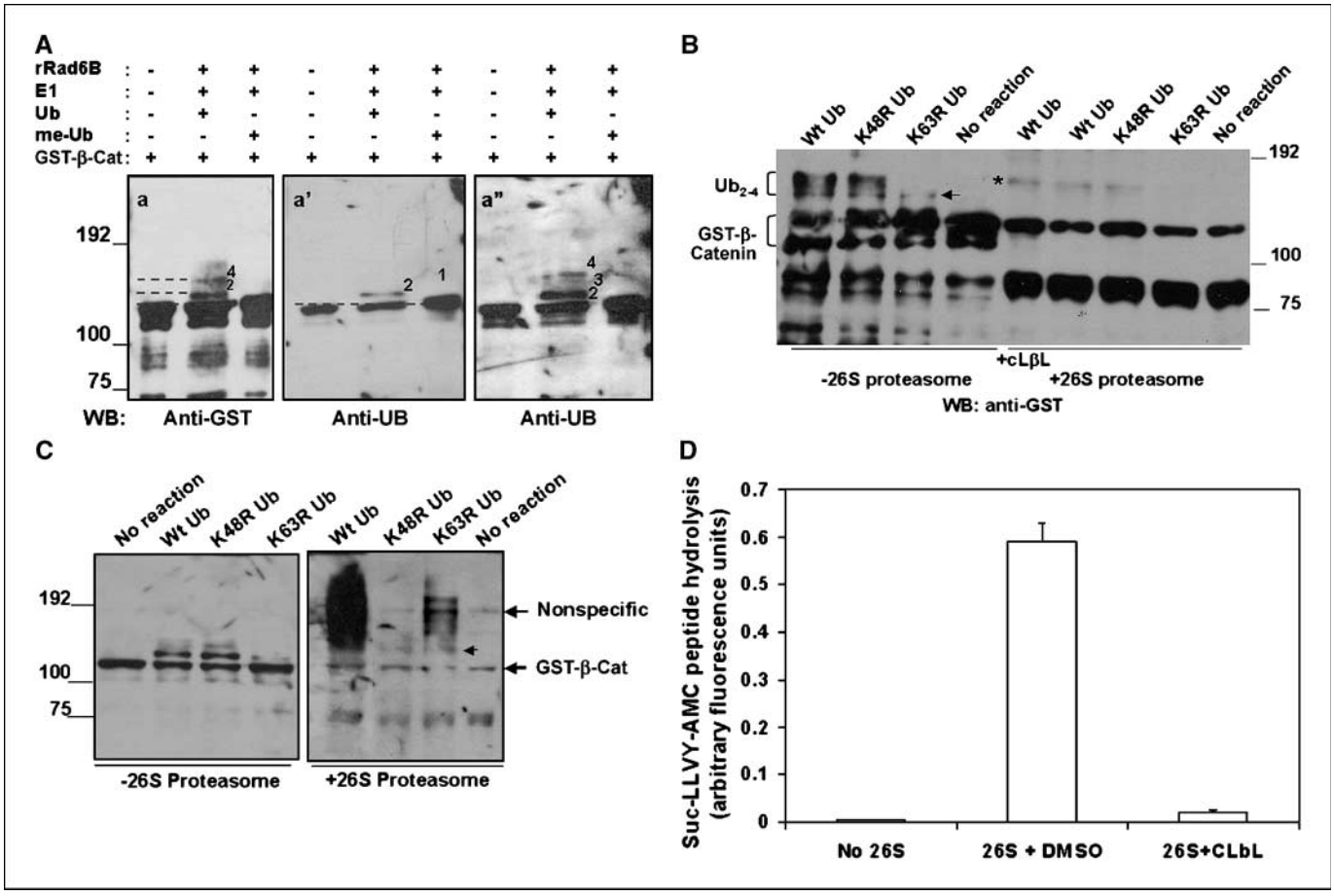

Figure 6. β-catenin is a substrate of Rad6B-mediated ubiquitination. *A,* ubiquitination reactions were performed with GST–β-catenin and rRad6B in presence of wild-type (*Ub*) or methylated Ub (*me-Ub*). Reaction products were analyzed by Western blotting with GST (*a*) or Ub (*a′* and *a″*) antibody. *a″* is a longer exposure of *a′*. *Horizontal lines,* the positions of ubiquitinated β-catenin conjugates containing one to four ubiquitin molecules. *B* and *C,* reactions performed in presence of wild-type, K48R, or K63R mutant ubiquitin. One-tenth of reaction mixtures containing ubiquitinated β-catenin products generated by rRad6B, or input GST–β-catenin substrate (*no reaction*) were incubated with 26S proteasome fraction or 26S proteasome fraction preincubated with CLβL. Reactions were analyzed by Western blotting with GST (*B*) or ubiquitin (*C*) antibodies. *Arrowhead,* the positions of GST-reactive ubiquitin conjugate in K63R ubiquitin reaction (*B*); *, GST-reactive ubiquitin conjugate generated in wild-type and K48R ubiquitin reactions after incubation with 26S proteasome(*B*). *Arrowhead,* the corresponding ubiquitin reactive band is indicated (*C*). Note intense reactivity to ubiquitin antibody in reactions containing wild-type or K63R ubiquitin and not K48R ubiquitin after incubation with 26S protasome fraction (*C*). *D,* failure to hydrolyze ubiquitin–β-catenin is not due to deficiency of proteasome activity as it hydrolyzes the fluorogenic peptide substrate Suc-LLVY-AMC. Specificity was determined in reactions that were preincubated with a 10-fold molar excess of cLβL. *Columns,* mean from two independent experiments; *bars,* SE.

overexpression, as a similar relationship between endogenous Rad6B and β-catenin is observed in WS-15 and MDA-MB-231 human breast cancer cells and in the MMTV-Wnt-1 mammary tumor model. These data suggest that Rad6B is a physiologic regulator of β-catenin ubiquitination and stability, and that the increased Rad6B frequently observed in breast carcinomas could contribute to β-catenin ubiquitination and stabilization. A detailed characterization of β-catenin distribution in the subcellular fractions of high and low Rad6B-expressing cells revealed significant differences in β-catenin modifications between the membrane, cytoplasmic, and nuclear fractions, although all fractions contained similar amounts of the nascent 90-kDa β-catenin protein. The presence of distinct high Mr β-catenin species suggests the operation of novel stabilizing mechanisms that include posttranslational ubiquitin modifications and implicate a uniquely modified nuclear β-catenin in regulation of β-catenin–mediated transcriptional activity. In support of the latter hypothesis, ChIP experiments showed that although unmodified β-catenin is present in the chromatin immunoprecipitates of both MCF10A and MDA-MB-231 cells, ubiquitinated β-catenin is efficiently immunoprecipitated only from MDA-MB-231 cells. These findings are consistent with our previous data that showed formation of β-catenin/TCF-4/Rad6B promoter complexes from MDA-MB-231 but not MCF10A nuclear proteins (13). Our present observation of ubiquitinated β-catenin in ChIPs of only MDA-MB-231 cells further support our notion that ubiquitinated β-catenin may be an important component of the β-catenin/TCF-4 transcriptional complex. In agreement, Rad6B RNAi decreased β-catenin–mediated transcriptional activity. Furthermore, Rad6B suppression in Wnt-1 tumor–derived G177 cells caused down-regulation of β-catenin ubiquitination and transcriptional activity, signifying a more general role for Rad6B in β-catenin modification and stabilization.

Rad6 is known to attach ubiquitin directly to a substrate protein with or without the help of an ubiquitin ligase (33). Results from *in vitro* ubiquitination assays using methylated ubiquitin show that Rad6B mediates addition of ubiquitin moieties to limited lysine residues on the β-catenin molecule, and chain extensions occur via K63R linkages. Because polyubiquitin chains involving K63 linkages, unlike K48 chains, do not play a role in protein turn over but are implicated in many cellular processes (34), our data implicate a novel role for Rad6B-generated K63 ubiquitin–β-catenin conjugates. Our observations suggest that the presence of Rad6B-initiated K63 extensions render the ubiquitin–β-catenin conjugates insensitive to proteasomes, or that the piling of ubiquitinated products induced in reactions containing 26S proteasome fraction is inhibitory to proteasomes. Our data from cycloheximide experiments confirmed that Rad6B specifically influences the stability of high Mr β-catenin as a sharp decline in high Mr β-catenin is observed in Rad6B-silenced WS-15 cells.

β-catenin is a target of phosphorylation by GSK3β, and phosphorylated DSGXXS motifs on β-catenin serve as signals for ubiquitination by βTrCP (35). β-catenin ubiquitination was unaffected by mutation of either K19 or K49, whereas double K19/K49 mutation showed residual βTrCP-dependent ubiquitination, and S33Y mutant β-catenin protein, which fails to bind βTrCP1/2, showed no βTrCP-mediated ubiquitination (36, 37). Ectopic expression of a dominant-negative βTrCP1 in HEK293 cells was found to potently inhibit monoubiquitination of wild-type, K19, K49, K19/K49, and S33Y mutant β-catenin but maintained similar levels of polyubiquitinated species (37). Our Western blotting data using dephospho-β-catenin antibody showed that a considerable proportion of β-catenin in MCF10A-Rad6B cells is unphosphorylated, yet stably ubiquitinated, suggesting the presence of novel ubiquitin modifying mechanisms that are independent of GSK3β. Because Rad6B silencing can suppress β-catenin monoubiquitination and polyubiquitination, our data implicate Rad6B as an important player in β-catenin modification. However, it is not known at present whether specific combinatorial interactions between the E2, Rad6B, and certain E3 ligases determine the stability of modified β-catenin.

In summary, this report establishes a novel mechanistic role for Rad6B in stabilization and activation of β-catenin in breast cancer cells. Our findings implicate the potential therapeutic value of Rad6B silencing in breast cancer subsets that exhibit autocrine Wnt signaling.

Acknowledgments

Received 6/6/2007; revised 10/16/2007; accepted 1/17/2008.

Grant support: Department of Defense Grants DAMD 17-02-0618, W81XWH07-1-0562 (M.P.V. Shekhar), and funding from Karmanos Cancer Institute and Wayne State University.

The costs of publication of this article were defrayed in part by the payment of page charges. This article must therefore be hereby marked *advertisement* in accordance with 18 U.S.C. Section 1734 solely to indicate this fact.

We thank Dr. Charlotte Lindvall and Cassandra Zylstra for assistance with G177 cells and MMTV-Wnt1 tumor sections, and Dr. Gloria Heppner for critical input and discussion of the manuscript.

References

1. Lawrence CW. The Rad6 DNA repair pathway in *Saccharomyces cerevisiae*: What does it do, and how does it do it? BioEssays 1994;16:253–8.
2. Reynolds P, Weber S, Prakash L. *Rad6* gene of *Saccharomyces cerevisiae* encodes a protein containing a tract of 13 consecutive aspartates. Proc Natl Acad Sci U S A 1985;82:168–72.
3. Jentsch S, McGrath JP, Varshavsky A. The yeast DNA repair *Rad6* encodes a ubiquitin conjugating enzyme. Nature 1987;329:131–4.
4. Haynes RH, Kunz BA. Life cycle and inheritance. In: Strathern J, Jones E, Broach J, editors. The Molecular Biology of the yeast *Saccharomyces cerevisiae*. Cold Spring Harbor: Cold Spring Harbor Laboratory; 1981. p. 371–414.
5. Lawrence CW. Mutagenesis in *Saccharomyces cerevisiae*. Adv Genet 1982;21:173–254.
6. Prakash S, Sung P, Prakash L. Structure and Function of *RAD3, RAD6,* and other DNA repair genes of *Saccharomyces cerevisiae*. In: Strauss PR, Wilson SH, editors. The Eukaryotic nucleus. Caldwell (NJ): Telford Press; 1990. Vol. 1, p. 275–92.
7. Sung P, Prakash S, Prakash L. Mutation of cysteine-88 in the *Saccharomyces cerevisiae* RAD6 protein abolishes its ubiquitin-conjugating activity and its various biological functions. Proc Natl Acad Sci U S A 1990;87:2695–9.
8. Sung P, Prakash S, Prakash L. Stable ester conjugates between the *Saccharomyces cerevisiae* RAD6 protein and ubiquitin has no biological activity. J Mol Biol 1991; 221:745–9.
9. Koken MHM, Reynolds P, Jaspers-Dekker I, et al. Structural and functional conservation of two human homologs of the yeast DNA repair gene *Rad6*. Proc Natl Acad Sci USA 1991;88:8865–9.
10. Koken MH, Smit EM, Jaspers-Dekker I, et al. Localization of two human homologs, *HHR6A* and *HHR6B*, of the yeast DNA repair gene *Rad6* to chromosomes Xq24–25 and 5q23–31. Genomics 1992;12:447–53.
11. Roest HP, Baarends WM, de Wit J, et al. The ubiquitin-conjugating DNA repair enzyme HR6A is a maternal factor essential for early embryonic development in mice. Mol Cell Biol 2004;24:5485–95.
12. Shekhar MP, Lyakhovich A, Visscher DW, Heng H, Kondrat N. RAD6 overexpression induces centrosome amplification, abnormal mitosis, aneuploidy and transformation. Cancer Res 2002;62:2115–24.
13. Shekhar MP, Tait L, Gerard B. Essential role of TCF/β-catenin in regulation of Rad6B expression: a potential mechanism for Rad6B overexpression in breast cancer cells. Mol Cancer Res 2006;4:729–45.
14. Reya T, Clevers H. Wnt signalling in stem cells and cancer. Nature 2005;434:843–50.
15. Wagenaar RA, Crawford HC, Matrisian LM. Stabilized β-catenin immortalizes colonic epithelial cells. Cancer Res 2001;61:2097–104.
16. Polakis P. Wnt signaling and cancer. Genes Dev 2000; 14:1837–51.
17. Cadigan KM, Nusse R. Wnt signaling: a common

theme in animal development. Genes Dev 1997;11: 3286–305.
18. Roura S, Miravet S, Piedra J, Garcia de Herreros A, Dunach M. Regulation of E-cadherin/Catenin association by tyrosine phosphorylation. J Biol Chem 1999;274: 36734–40.
19. Brennan KR, Brown AM. Wnt proteins in mammary development and cancer. J Mammary Gland Biol Neoplasia 2004;9:119–31.
20. Nusse R,Varmus HE. *Wnt* genes. Cell 1992;69:1073–87.
21. Tsukamoto AS, Grosschedl R, Guzman RC, Parslow T, Varmus HE. Expression of the int-1 gene in transgenic mice is associated with mammary gland hyperplasia and adenocarcinomas in male and female mice. Cell 1988;55:619–25.
22. Pauley RJ, Santner SJ, Tait LR, Bright RK, Santnen RJ. Regulated CYP19 aromatase transcription in breast stromal fibroblasts. J Clin Endocrinol Metab 2000;85: 837–46.
23. Lyakhovich A, Shekhar MP. Supramolecular complex formation between Rad6 and proteins of p53 pathway during DNA damage-induced response. Mol Cell Biol 2003;23:2463–75.
24. Bafico A, Liu G, Goldin L, Harris V, Aaronson SA. An autocrine mechanism for constitutive Wnt pathway activation in human cancer cells. Cancer Cell 2004;6: 497–506.
25. Robzyk K, Recht J, Osley MA. Rad6-dependent ubiquitination of histone H2B in yeast. Science 2000; 287:501–4.
26. Shtutman M, Zhurinsky J, Simcha I, et al. The cyclin D1 gene is a target of the β-catenin/LEF-1 pathway. Proc Natl Acad Sci U S A 1999;96:5522–7.
27. Michaelson JS, Leder P. β-catenin is a downstream effector of Wnt-mediated tumorigenesis in the mammary gland. Oncogene 2001;20:5093–9.
28. Li Y, Welm B, Podsypanina K, et al. Evidence that transgenes encoding components of the Wnt signaling pathway preferentially induce mammary cancers from progenitor cells. Proc Natl Acad Sci U S A 2003;100: 15853–8.
29. Xie Y, Varshavsky A. Physical association of ubiquitin ligases and the 26S proteasome. Proc Natl Acad Sci USA 2000;97:2497–502.
30. Howe LR, Brown AM. Wnt signaling and breast cancer. Cancer Biol Ther 2004;3:36–41.
31. Brown AM. Wnt signaling in breast cancer: Have we come full circle? Breast Cancer Res 2001;3:351–5.
32. Candidus S, Bischoff P, Becker KF, Hofler H. No evidence for mutations in the α- and β- catenin genes in human gastric and breast carcinomas. Cancer Res 1996; 56:49–52.
33. Sung P, Prakash S, Prakash L. The RAD6 protein of *Saccharomyces cerevisiae* polyubiquitinates histones, and its acidic domain mediates this activity. Genes Dev 1988;2:1476–85.
34. Pickart CM, Fushman D. Polyubiquitin chains: polymeric protein signals. Curr Opin Chem Biol 2004;8:610–6.
35. Kitagawa M, Hatakeyama S, Shirane M, et al. An F-box protein, FWD1, mediates ubiquitin- dependent proteolysis of β-catenin. EMBO J 1999;18:2401–10.
36. Aberle H, Bauer A, Stappert J, Kispert A, Kemler R. β-catenin is a target for the ubiquitin- proteasome pathway. EMBO J 1997;16:3797–804.
37. Winer IS, Bommer GT, Gonik N, Fearon ER. Lysine residues Lys-19 and Lys-49 of β-catenin regulate its levels and function in T cell factor transcriptional activation and neoplastic transformation. J Biol Chem 2006;281:26181–7.